

Rechargeable Li/CO<sub>2</sub>-O<sub>2</sub> (2 : 1) battery and Li/CO<sub>2</sub> battery†

Yali Liu, Rui Wang, Yingchun Lyu, Hong Li\* and Liquan Chen

Cite this: *Energy Environ. Sci.*, 2014, 7, 677Received 6th October 2013  
Accepted 8th November 2013

DOI: 10.1039/c3ee43318h

www.rsc.org/ees

A Li/CO<sub>2</sub>-O<sub>2</sub> (2 : 1, volume ratio) battery and a Li/CO<sub>2</sub> battery with discharging specific capacities of 1808 mA h g<sup>-1</sup> and 1032 mA h g<sup>-1</sup>, respectively, are reported. Li<sub>2</sub>CO<sub>3</sub> is the main discharge product in the Li/CO<sub>2</sub>-O<sub>2</sub> (2 : 1) battery and can be decomposed during charging. In the Li/CO<sub>2</sub> battery, the main discharge products could be Li<sub>2</sub>CO<sub>3</sub> and carbon. Both batteries can be cycled reversibly at room temperature.

## 1 Introduction

Rechargeable nonaqueous lithium-air batteries have attracted wide attention due to their very high theoretical energy density.<sup>1-3</sup> It is still a challenge to operate the batteries in air due to the influence of moisture and carbon dioxide.<sup>2,4,5</sup> It has been demonstrated that there would be Li<sub>2</sub>CO<sub>3</sub> in the discharge products when the reactive gas contains CO<sub>2</sub>, and Li<sub>2</sub>CO<sub>3</sub> is difficult to be decomposed during charging.<sup>6</sup> Therefore, most reported lithium air batteries are investigated under high pure oxygen with CO<sub>2</sub> less than 5 ppm. In 2011, K. Takechi *et al.* reported a Li/CO<sub>2</sub>-O<sub>2</sub> (from 0 to 100% volume CO<sub>2</sub>) battery, which didn't show a reversible charge capacity with a cut-off voltage of 4.5 V even in the first cycle.<sup>6</sup> B. D. McCloskey *et al.* reported a Li/O<sub>2</sub> battery with CO<sub>2</sub> as a contamination gas (10% volume). This battery employed LiTFSI-DME as electrolyte and a sloped charging voltage profile up to 4.8 V was reported only in the first cycle.<sup>5</sup> A reversible Li/CO<sub>2</sub>-O<sub>2</sub> (1 : 1, volume ratio) battery with DME based and DMSO based electrolytes was

Beijing National Laboratory for Condensed Matter Physics, Institute of Physics, Chinese Academy of Sciences, Beijing, 100190, P.R. China. E-mail: hli@iphy.ac.cn; Fax: +86 10 82649046; Tel: +86 10 82648067

† Electronic supplementary information (ESI) available: The elemental constituents of the pristine, first discharge, first charge, fifth discharge and fifth charge. The charge and discharge curves of the battery with Ar as working gas. The cyclic voltammetry curves and FTIR spectra of electrolyte. <sup>7</sup>Li NMR spectra of the KB electrode in the pristine, first discharge and charge state. The charge and discharge curves of Li/CO<sub>2</sub> battery with porous Au as cathode, TEM and EELS of the porous gold electrode in the first discharge state in the Li/CO<sub>2</sub> battery. DOI: 10.1039/c3ee43318h

### Broader context

The successful development of a Li air battery has been greatly anticipated due to its highest theoretical energy density among all electrochemical energy storage devices. Many challenges are still remaining. One of the technical barriers is the formation of stable Li<sub>2</sub>CO<sub>3</sub> partially due to the existence of CO<sub>2</sub> in the air. Consequently, the main research activities are focusing on Li/O<sub>2</sub> batteries without CO<sub>2</sub>. In addition, CO<sub>2</sub> capture and utilization are also essential topics. Here we report that it is possible to develop rechargeable Li/CO<sub>2</sub>-O<sub>2</sub> (2 : 1, volume ratio) batteries and even Li/CO<sub>2</sub> batteries.

reported by H. Kim and K. Kang very recently.<sup>7</sup> They pointed out that Li<sub>2</sub>CO<sub>3</sub> was the main discharge product in this battery and can form reversibly. We have also reported that Li<sub>2</sub>CO<sub>3</sub> can be decomposed after mixing with NiO as catalyst.<sup>8</sup> Accordingly, we believe that the formed Li<sub>2</sub>CO<sub>3</sub> can be decomposed under suitable conditions. Therefore, it is plausible that a rechargeable Li/CO<sub>2</sub> battery could be developed. According to thermodynamic calculations, the specific energy density of Li/CO<sub>2</sub> batteries is almost three fourths of a Li/O<sub>2</sub> battery.<sup>9</sup> It also can be calculated that the theoretical voltage is about 2.8 V based on the equation: 4Li + 3CO<sub>2</sub> → 2Li<sub>2</sub>CO<sub>3</sub> + C. Li/CO<sub>2</sub> batteries could be attractive especially when CO<sub>2</sub> is enriched in the atmosphere. Previously, Archer *et al.* reported a primary Li/CO<sub>2</sub> battery which cannot be recharged and only discharges at high temperature.<sup>10</sup> In this communication, we demonstrate that a Li/CO<sub>2</sub>-O<sub>2</sub> (2 : 1, volume ratio) battery and a Li/CO<sub>2</sub> battery can operate reversibly at room temperature when lithium triflate (LiCF<sub>3</sub>SO<sub>3</sub>)-TEGDME is used as the electrolyte.

## 2 Experimental section

High pure anhydrous LiCF<sub>3</sub>SO<sub>3</sub> (≥99.995%, Sigma Aldrich Co.) was used as received. TEGDME (≥99%, Sigma Aldrich Co.) was purchased and dehydrated with 0.3 nm molecular sieves (Metrohm Ltd., Switzerland). Then, LiCF<sub>3</sub>SO<sub>3</sub> was dissolved in TEGDME in a molar ratio of 1 : 4 to form the electrolyte. The cathode composition was Ketjen Black (KB) and PTFE

(Polytetrafluoroethylene preparation, 60% dispersion in H<sub>2</sub>O, Sigma Aldrich Co.) at a weight ratio of 90 : 10. Then the cathode mixture was rolled onto the stainless steel mesh (80 meshes) and dried at 110 °C under vacuum for 8 h. Glass fiber (Whatman) was used as the separator. All the manipulations sensitive to moisture were performed in an argon atmosphere glove box (MBraun, H<sub>2</sub>O and O<sub>2</sub> < 0.1 ppm).

After assembly, the battery was put into a glass container and piped into the reactant gas (CO<sub>2</sub>-O<sub>2</sub> = 2 : 1 in volume ratio or pure CO<sub>2</sub>). Charge–discharge tests were carried out on a Land Battery Testing System and performed *via* a galvanostatic method. Before the measurements of the next step, the battery was disassembled and the cathode electrode was washed by 1,2-dimethoxyethane ( $\geq 99\%$ , Alfa Aesar).

X-ray diffraction (XRD) was performed on a Bruker D8 Advance X-ray Diffractometer using Cu K $\alpha$ 1 radiation ( $\lambda = 1.5405 \text{ \AA}$ ). In the XRD measurement, the cathode electrode was coated by a Kapton film to avoid exposing to air. Fourier transform infrared (FTIR) spectra were collected from a Bruker Vertex 70v infrared spectroscopy. The FTIR spectrum was recorded in the range of 1850–400 cm<sup>-1</sup>. The preparation of the sample was carried out in the glove box before measurements. The morphologies of electrode plates were observed by a Hitachi S-4800 scanning electron microscope (SEM). The samples were sealed in a special vacuum transfer box during sample transfer from the glove box to the SEM chamber.

### 3 Results and discussion

#### 3.1 Charge and discharge voltage profiles

Charge and discharge voltage profiles of the Li/O<sub>2</sub> battery, Li/CO<sub>2</sub>-O<sub>2</sub> (2 : 1) battery and Li/CO<sub>2</sub> battery at the same current density (30 mA g<sup>-1</sup>, about 0.1 mA cm<sup>-2</sup>) using stainless steel meshes as current collectors are shown in Fig. 1. The discharge profiles are similar for the three batteries. The Li/CO<sub>2</sub>-O<sub>2</sub> (2 : 1) battery shows the highest discharge voltage at 2.75 V vs. Li<sup>+</sup>/Li.

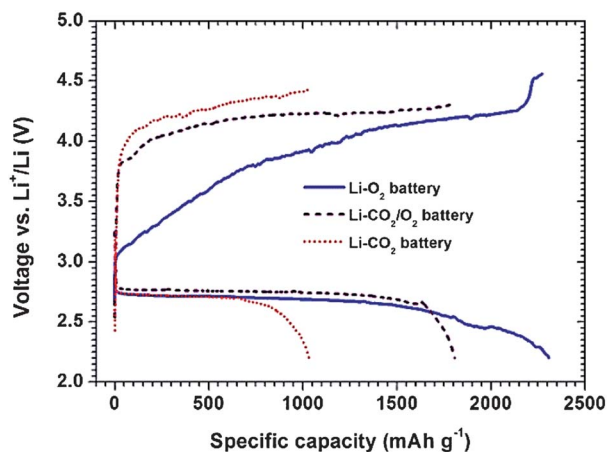


Fig. 1 The charge–discharge curves of Li/O<sub>2</sub> battery (solid line), Li/CO<sub>2</sub>-O<sub>2</sub> (2 : 1 in volume ratio) battery (dash line) and Li/CO<sub>2</sub> battery (dot line). The cut-off voltage of discharge is 2.2 V. The current density is 30 mA g<sup>-1</sup>. The cathode is KB and PTFE at a weight ratio of 90 : 10.

The voltage profiles of the Li/CO<sub>2</sub>-O<sub>2</sub> (2 : 1) battery and Li/CO<sub>2</sub> battery during the first charge is different to that of the Li/O<sub>2</sub> battery. The latter shows a slope while the other two systems show mainly a high voltage plateau above 4.0 V vs. Li<sup>+</sup>/Li, implying higher polarization of the CO<sub>2</sub>-based batteries during charging. Whether this difference is caused by thermodynamic or kinetic factors needs future clarification. The reversible discharge specific capacities are 2273 mA h g<sup>-1</sup>, 1808 mA h g<sup>-1</sup> and 1032 mA h g<sup>-1</sup>, respectively based on the weight of Ketjen Black. Different with the reports by Takechi and Archer *et al.*,<sup>6,10</sup> both the Li/CO<sub>2</sub>-O<sub>2</sub> (2 : 1) battery and Li/CO<sub>2</sub> battery can be recharged. It seems that the main difference in the electrolyte plays a key role.

For comparison, the charge and discharge performance of a battery with Ar as working gas were also tested. The result is shown in Fig. S1 (ESI<sup>†</sup>). It can be seen that there was almost no capacity in this battery. Besides, the electrolyte is stable up to 4.38 V in all the Ar, CO<sub>2</sub>, O<sub>2</sub> and CO<sub>2</sub>-O<sub>2</sub> (2 : 1) mixture atmospheres, which were shown in the cyclic voltammetry in Fig. S2.†

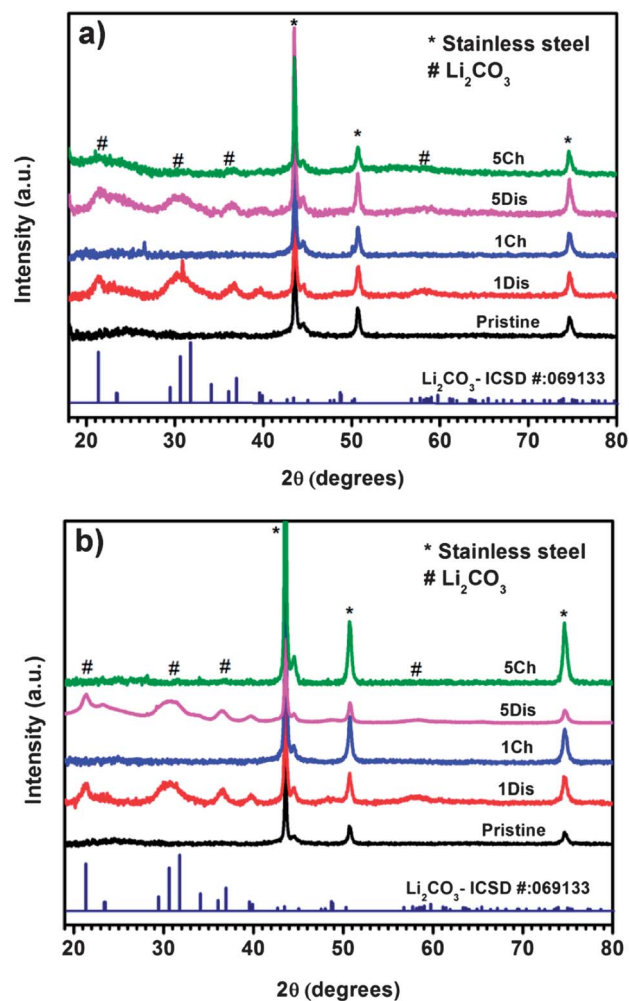


Fig. 2 The XRD pattern of a pristine KB electrode, the first discharge, first charge, fifth discharge and fifth charge state in (a) Li/CO<sub>2</sub>-O<sub>2</sub> (2 : 1) battery and (b) Li/CO<sub>2</sub> battery. The reference pattern for Li<sub>2</sub>CO<sub>3</sub> is also shown.

Besides, the stability of the electrolyte upon oxygen reduction is conducted by  $^7\text{Li}$  NMR (shown in Fig. S3†). It can be seen that the electrolyte is relatively stable, at least in the first cycle.

### 3.2 Charge and discharge products analysis

XRD analysis for the KB electrode at the complete discharge and charge states has been performed. It can be seen in Fig. 2a that  $\text{Li}_2\text{CO}_3$  is the main discharge product in the  $\text{Li}/\text{CO}_2\text{-O}_2$  (2 : 1) battery after the first discharge. The patterns corresponding to  $\text{Li}_2\text{CO}_3$  disappear after the first charge, indicating a reversible process. After the fifth discharge,  $\text{Li}_2\text{CO}_3$  is still the main product. However, it seems that the peaks of  $\text{Li}_2\text{CO}_3$  do not disappear completely after the fifth charging. The mechanism of the lower reversibility after the fifth cycle needs further clarification. The XRD patterns of the KB cathode in the  $\text{Li}/\text{CO}_2$  battery are shown in Fig. 2b. The results are quite similar to the  $\text{Li}/\text{CO}_2\text{-O}_2$  (2 : 1) battery except for that  $\text{Li}_2\text{CO}_3$  disappears completely after the fifth charging. No other phase can be identified in both cases. All these results are supported by the element constituent analyses which are shown in Table S1 and S2.†

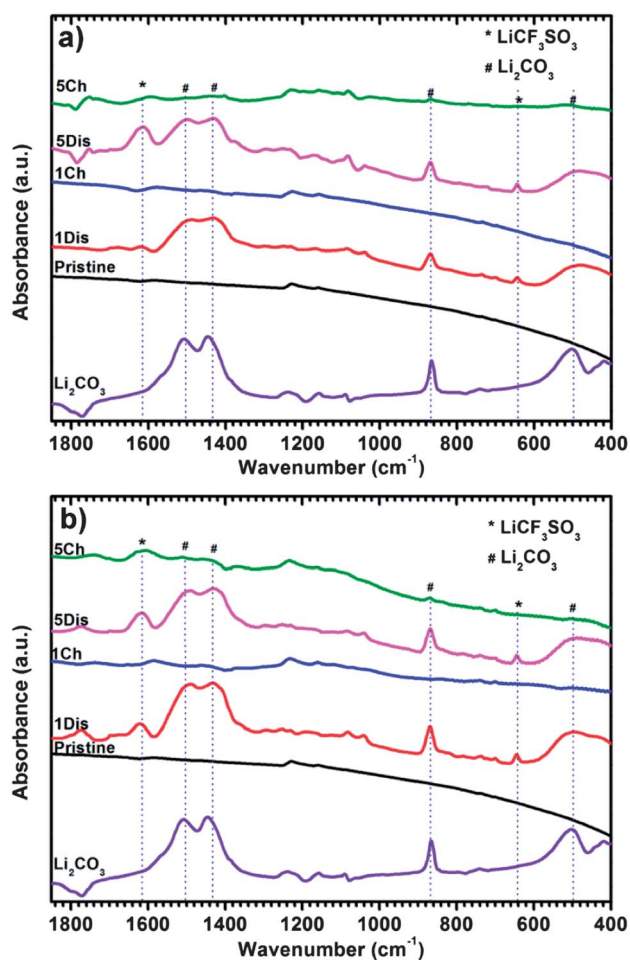


Fig. 3 The FTIR spectra of pristine KB electrode, the first discharge, first charge, fifth discharge and fifth charge state in (a)  $\text{Li}/\text{CO}_2\text{-O}_2$  (2 : 1) battery and (b)  $\text{Li}/\text{CO}_2$  battery. The reference spectra for  $\text{Li}_2\text{CO}_3$  are also shown.

The FTIR spectra of the  $\text{Li}/\text{CO}_2\text{-O}_2$  (2 : 1) battery and the  $\text{Li}/\text{CO}_2$  battery at different discharge and charge states are shown in Fig. 3a and b, respectively. In both cases, reversible formation and decomposition of the  $\text{Li}_2\text{CO}_3$  phase can be seen clearly from the appearance and disappearance of the vibration modes around  $868\text{ cm}^{-1}$ ,  $1431\text{ cm}^{-1}$  and  $1505\text{ cm}^{-1}$ . Other peaks belong to  $\text{LiCF}_3\text{SO}_3$  in the electrolyte (shown in Fig. S4†). They are more apparent in the discharge state for the reason that the surface of the discharged electrode is rougher and there will be more lithium salts residue.

The top view SEM images of the cathode electrode plates in the discharged and charged states in the first and fifth cycle of the  $\text{Li}/\text{CO}_2\text{-O}_2$  (2 : 1) battery and the  $\text{Li}/\text{CO}_2$  battery are shown in Fig. 4. It can be seen that the pristine electrode is composed of agglomerated KB particles with size of 30–50 nm. At the discharge states, mesh-like fibre products covered the surface. Comparing the  $\text{Li}/\text{CO}_2\text{-O}_2$  (2 : 1) battery to the  $\text{Li}/\text{CO}_2$  battery, the discharge product of the former seems looser than the later. Compared to the literatures of  $\text{Li-O}_2$  batteries using KB as air cathode,<sup>7,11</sup> the products in the  $\text{CO}_2$  based battery do not form particles but a layer on the surface of the cathode. It seems that the morphology of the observed products is related to the reaction with  $\text{CO}_2$ .

In order to confirm the existence of carbon, porous gold was used as a cathode in the  $\text{Li}/\text{CO}_2$  battery. The preparation of porous gold followed the method in the literature.<sup>12</sup> The charge and discharge curves (shown in Fig. S5†) of the  $\text{Li}/\text{CO}_2$  battery with porous gold as cathode are similar to the battery with KB as cathode. Then by surface enhanced Raman spectroscopy (shown in Fig. S6†) and electron energy loss spectroscopy (shown in Fig. S7†), amorphous carbon was observed. It is not clear whether the reaction mechanism is the same in  $\text{Li}/\text{CO}_2$  batteries with porous Au and KB as cathode respectively. Thus, the results with porous gold as cathode are used as reference.

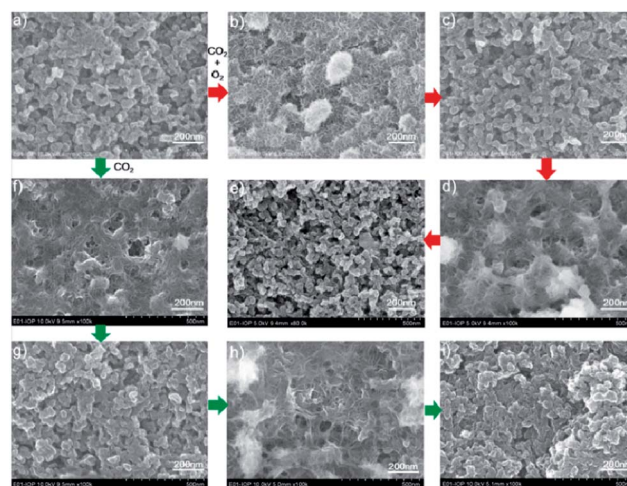


Fig. 4 SEM images of (a) pristine KB electrode, (b) electrode plate in the first discharge, (c) first charge, (d) fifth discharge and (e) fifth charge state in the  $\text{Li}/\text{CO}_2\text{-O}_2$  (2 : 1) battery. (f–i) correspond to the  $\text{Li}/\text{CO}_2$  battery.

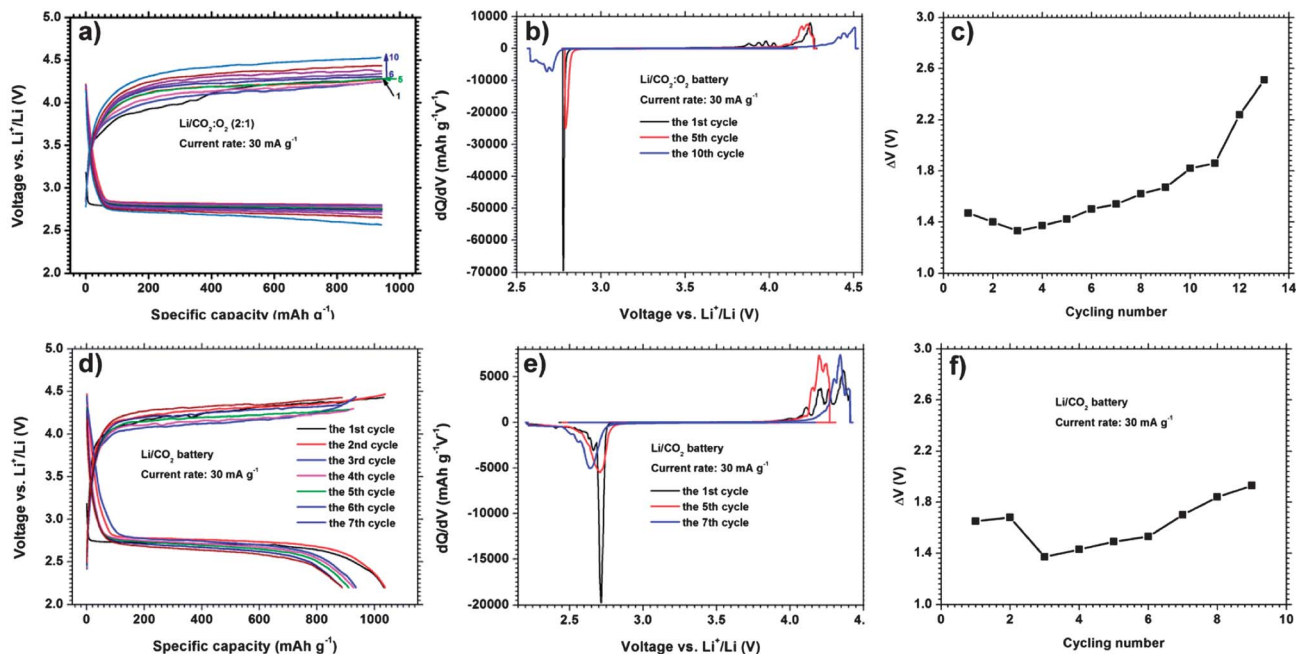


Fig. 5 (a) Charge–discharge voltage profiles of the Li/CO<sub>2</sub>–O<sub>2</sub> (2 : 1) battery with fixed capacity, (b) differential capacity curve and (c) voltage hysteresis between the charging and discharging curves of the Li/CO<sub>2</sub>–O<sub>2</sub> (2 : 1) battery. (d) Charge–discharge voltage profiles of the Li/CO<sub>2</sub> battery with cut-off voltage of 2.2 V, (e) differential capacity curve and (f) voltage hysteresis between the charging and discharging curves of the Li/CO<sub>2</sub> battery. The current densities of both batteries are 30 mA g<sup>-1</sup>.

### 3.3 Cycling performance

The voltage profiles,  $dQ/dV$  profiles and polarization voltage of the Li/CO<sub>2</sub>–O<sub>2</sub> (2 : 1) battery are shown in Fig. 5a–c, respectively. The current rate and specific capacity of the battery are set to 30 mA g<sup>-1</sup> (about 0.1 mA cm<sup>-2</sup>) and 1000 mA h g<sup>-1</sup>, respectively. In this measurement the capacity limit was utilized for the reason that it is beneficial to promote cycling performance. It is known that the conductivity of Li<sub>2</sub>O<sub>2</sub> is low.<sup>13,14</sup> J. M. Garcia-Lastra *et al.* pointed out that the charge transport of Li<sub>2</sub>CO<sub>3</sub> was even poorer than Li<sub>2</sub>O<sub>2</sub>.<sup>15</sup> As a result, if full discharge was conducted, the impedance of the battery will become so large that it is difficult to decompose the discharge products. It can be seen that the battery can operate reversibly and the platform voltages in the charging process are no higher than 4.3 V in the first five cycles. From these figures it can be calculated that the round trip efficiency of the Li/CO<sub>2</sub>–O<sub>2</sub> (2 : 1) battery is about 66.7%. In addition, it also can be observed that the over potential increases with the cycling number growing, which may be related to the accumulation of inactive Li<sub>2</sub>CO<sub>3</sub>.

The charge and discharge profiles, differential capacities and polarization voltage of the Li/CO<sub>2</sub> battery are shown in Fig. 5d–f. In Fig. 5d, the battery was discharged to 2.2 V and then recharged to the same specific capacity and discharged under a current density of 30 mA g<sup>-1</sup>. The same phenomenon as the Li/CO<sub>2</sub>–O<sub>2</sub> (2 : 1) battery can be seen from these figures. Besides, the polarization of the Li/CO<sub>2</sub> battery is a little larger than the Li/CO<sub>2</sub>–O<sub>2</sub> (2 : 1) battery and the round trip efficiency is a little lower (66.3%).

In any case, the Li–air battery based on high concentration CO<sub>2</sub> can operate over tens of cycles without any catalyst and

special cathode material. It is believed that the electrochemical performances could be improved after further comprehensive optimization.

## 4 Conclusions

Our preliminary investigations indicate that the Li/CO<sub>2</sub>–O<sub>2</sub> (2 : 1) battery and the Li/CO<sub>2</sub> battery can discharge and charge reversibly using LiCF<sub>3</sub>SO<sub>3</sub> in TEGDME (1 : 4 in mole) as the electrolyte. In both cases, Li<sub>2</sub>CO<sub>3</sub> is the main product and can be decomposed reversibly. The reaction products show a network of fibres covered on the surface. The round trip efficiency is about 66.7% and 66.3%, respectively. The reaction mechanism, thermodynamic and kinetic properties are still not very clear, needing further investigation. Although the performances of the Li/CO<sub>2</sub>–O<sub>2</sub> (2 : 1) battery and the Li/CO<sub>2</sub> battery are far from applications, our new findings show the promising feature that greenhouse gas CO<sub>2</sub> could be captured and utilized as a valuable energy storage medium.

## Acknowledgements

Financial support from CAS project (KJXC2-YW-W26), "Strategic Priority Research Program" of the Chinese Academy of Sciences, Grant No. XDA01020304 and National project 973 (2012CB932900) are appreciated. The authors thank the help from Prof. Xuekui Xi, Mr Dongdong Xiao and Prof. L. Gu for NMR and TEM, EELS experiments.

## Notes and references

- 1 G. Girishkumar, B. McCloskey, A. C. Luntz, S. Swanson and W. Wilcke, *J. Phys. Chem. Lett.*, 2010, **1**, 2193–2203.
- 2 P. G. Bruce, S. A. Freunberger, L. J. Hardwick and J.-M. Tarascon, *Nat. Mater.*, 2012, **11**, 19–29.
- 3 K. M. Abraham and Z. Jiang, *J. Electrochem. Soc.*, 1996, **143**, 1–5.
- 4 S. Meini, M. Piana, N. Tsiouvaras, A. Garsuch and H. A. Gasteiger, *Electrochem. Solid State Lett.*, 2012, **15**, A45–A48.
- 5 S. R. Gowda, A. Brunet, G. M. Wallraff and B. D. McCloskey, *J. Phys. Chem. Lett.*, 2013, **4**, 276–279.
- 6 K. Takechi, T. Shiga and T. Asaoka, *Chem. Commun.*, 2011, **47**, 3463–3465.
- 7 H.-K. Lim, H.-D. Lim, K.-Y. Park, D.-H. Seo, H. Gwon, J. Hong, W. A. Goddard, H. Kim and K. Kang, *J. Am. Chem. Soc.*, 2013, **135**, 9733–9742.
- 8 R. Wang, X. Yu, J. Bai, H. Li, X. Huang, L. Chen and X. Yang, *J. Power Sources*, 2012, **218**, 113–118.
- 9 C. X. Zu, J. Y. Peng and H. Li, *Energy Storage Science and Technology*, 2013, **2**, 8.
- 10 S. Xu, S. K. Das and L. A. Archer, *RSC Adv.*, 2013, **3**, 6656–6660.
- 11 J. Xiao, D. Wang, W. Xu, D. Wang, R. E. Williford, J. Liu and J.-G. Zhang, *J. Electrochem. Soc.*, 2010, **157**, A487–A492.
- 12 Y. Ding, Y. J. Kim and J. Erlebacher, *Adv. Mater.*, 2004, **16**, 1897–1900.
- 13 M. D. Radin, J. F. Rodriguez, F. Tian and D. J. Siegel, *J. Am. Chem. Soc.*, 2011, **134**, 1093–1103.
- 14 O. Gerbig, R. Merkle and J. Maier, *Adv. Mater.*, 2013, **25**, 3129–3133.
- 15 J. M. Garcia-Lastra, J. S. G. Myrdal, R. Christensen, K. S. Thygesen and T. Vegge, *J. Phys. Chem. C*, 2013, **117**, 5568–5577.